

## An empirical algorithm to estimate silicate in the Southwest Bay of Bengal

K Priyanka<sup>a,b</sup>, R K Sarangi<sup>b</sup>, R Shanthi<sup>a</sup>, D Louwinanand<sup>a</sup> & A Saravanakumar<sup>\*a</sup>

<sup>a</sup>Centre of Advanced Study in Marine Biology, Annamalai University, Parangipettai, Tamil Nadu – 608 502, India

<sup>b</sup>Marine Ecosystem Division, BPSG/EPISA, Space Applications Centre (ISRO), Ahmedabad – 380 015, India

\*[E-mail: asarvaan@gmail.com]

Received 13 July 2022; revised 13 September 2023

Silicate is a significant prerequisite for the growth and development of primary producers, mainly in diatoms, it remains a prevalent contributor. Satellite ocean colour sensors data are broadly utilized for the identification, mapping and monitoring the phytoplankton characteristics, spatial and temporal. In this study, an empirical algorithm was developed for mapping the silicate concentration an important nutrient for planktonic diatoms depending on the relationship between chlorophyll-*a*, Sea Surface Temperature (SST) and silicate at a high spatio-temporal resolution. Three dimensional polynomial functions, such as plane, paraboloid, Gaussian and Lorentzian functions were used to correlate SST, chlorophyll-*a* and silicate. Among these the paraboloid function provided significant relationship between the variables with an  $R^2$  value of 0.828. Validation of Visible Infrared Imaging Radiometer Suite (VIIRS) derived SST ( $R^2 = 0.634$ , Mean Normalized Bias (MNB) = 0.006, Root Mean Square Error (RMSE) = 0.280 and Standard Error of Estimation (SEE) =  $\pm 0.227$ ) and chlorophyll-*a* ( $R^2 = 0.523$ , MNB = 0.369, RMSE = 0.846, and SEE =  $\pm 0.632$ ) observed better synchronization with *in situ* measurements of SST and chlorophyll-*a*, respectively. The VIIRS-derived silicate algorithm provided better agreements with *in situ* silicate concentration ( $R^2 = 0.784$ , MNB = -0.001, RMSE = 1.394 and SEE =  $\pm 0.839$ ) along the Southwest Bay of Bengal.

[**Keywords:** Bay of Bengal, Diatoms, Silicate algorithm, SNPP VIIRS, Chlorophyll-*a*, Sea surface temperature]

### Introduction

Nutrients play an important role in the development and diversity of phytoplankton, which may in turn reflect the ecological conditions of the marine environment<sup>1</sup>. The estimation of nutrient fluxes in the surface oceanic waters and their subsequent consumption by marine phytoplankton remains major challenge for oceanographers<sup>2</sup>. These nutrients such as nitrate, phosphate, silicate and trace metals are utilized by phytoplankton during photosynthesis<sup>3</sup>. The upwelling associated nutrient-rich cold water stimulates intense phytoplankton blooms mainly driven by diatoms. In the Bay of Bengal, the enrichment of silicate is higher compared to other micronutrients such as nitrate, nitrite, phosphate etc.<sup>4</sup>. The riverine input is the most important and potential source of nutrients in the Southwest (SW) Bay of Bengal (BoB). In contrast to other phytoplankton, diatoms which are abundant in tropical seas require silicate in large amounts for their growth<sup>5</sup>. Therefore, the extent of diatom blooms and their impact on primary production are influenced by the quantum of silicic acid carried to the euphotic zone during upwelling.

Diatoms are the major contributors to biosilicification and global carbon fixation<sup>1</sup>. In the euphotic zone, offshore upwelling system tends to obtain silicate-limited through differential export of deep water<sup>1</sup>. Zooplankton, which feeds upon diatoms prompts greater regeneration of nitrate than silicate. In the marine systems, silicate plays a vital role in the development of phytoplankton bloom<sup>6</sup> and diatoms have an absolute prerequisite for silicon<sup>5</sup> *i.e.* for the formation of cell valves and completing the cell cycle<sup>2,4</sup>.

In Bay of Bengal, phytoplankton diversity and species succession depend greatly on the seasonal variations associated with fluctuations in temperature and nutrient concentration<sup>7,8</sup>. As the fundamental correlations between temperature, nutrients, and chlorophyll are not highly stable, a combined data from multiple years is required to generate a single set of regression equations that can depict surface nitrate and silicate concentrations for each sub-region<sup>9</sup>. Hence, clear understanding on spatio-temporal changes in the silicate concentration along the SW BoB will provide important information on diatom productivity.

Henson *et al.*<sup>9</sup> utilized satellite data-based assessments of nitrate and silicate concentrations to investigate the timing of nutrient depletion and infer its impacts on species succession. In addition, the utilization of satellite imagery to forecast and simulate ocean productivity has gained increasing importance and acceptance in the recent years, as satellite sensors in the visible and infrared regions of the electromagnetic spectrum provide large spatial coverage and temporal repeatability<sup>2</sup>.

Several studies have been conducted on the seasonal variations of physico-chemical parameters and nutrients in the BoB<sup>7,10,11</sup>. Earlier investigations in the SW BoB have focused on developing algorithms for mapping nitrate as the major limiting nutrient through remote sensing<sup>2,12,13</sup>. However, the present study is mainly focused on i) the development of a silicate map to clarify the timing of silicate depletion and diatom dominance in the SW BoB, ii) to evaluate the validation of *in situ* Sea Surface Temperature (SST) and chlorophyll-*a* (chl-*a*) using the Visible Infrared Imaging Radiometer Suite (VIIRS), and iii) to validate the silicate map with *in situ* silicate measurements for accuracy.

### Materials and Methods

The surface water samples were collected monthly from the SW BoB over a period of five years (2013 to 2017) using 5-L Niskin water sampler at four sampling stations *viz.* Chennai (80°24'52.8" E; 13°54'14.4" N), Pondicherry (79°53'6" E; 11°24'7.2" N), Parangipettai (79°51'50.4" E; 11°54'7.2" N), and Nagapattinam (80°12'23.64" E; 10°46'35.76" N) at a distance of 1, 2, 3, 4 and 5 km from the coast at each sampling station in Figure 1.

#### *In situ* data

*In situ* Sea Surface Temperature (SST) was measured using a digital multi-sensor with an accuracy of ±0.01 °C (Merck Millipore-Multi 3420). The silicate concentration was determined by the molybdate method using an ultraviolet-visible spectrophotometer (Shimadzu-UV 2480)<sup>14</sup>. Chlorophyll-*a* was filtered using a 47 mm GF/F filter, extricated using 90 % acetone and determined with a Shimadzu UV 2480 spectrophotometer (Shimadzu, Inc., Tokyo)<sup>14</sup>.

#### Satellite data

The Visible Infrared Imaging Radiometer Suite (VIIRS) of the Suomi National Polar-orbiting Partnership (SNPP) satellite obtained a 1 km SST and

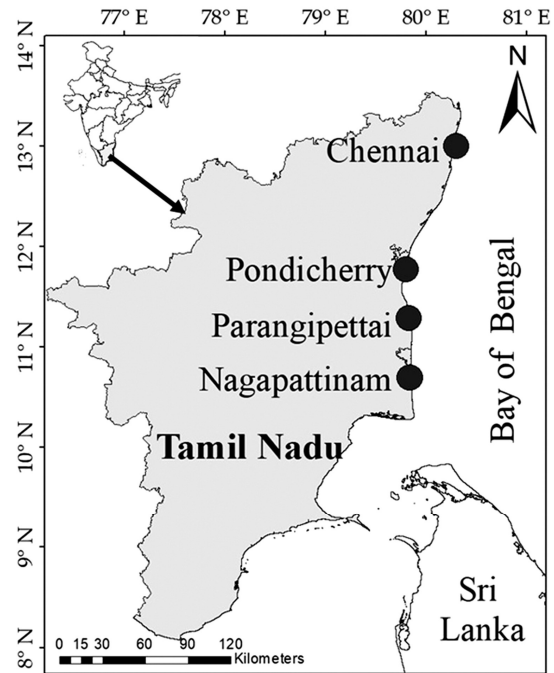


Fig. 1 — Study area map showing sampling stations in the SW Bay of Bengal water

chlorophyll-*a* images for 31<sup>st</sup> January 2017, which were obtained from the Ocean Color Web. The satellite-derived images were interpreted and analyzed using SeaDAS 7.4 software.

#### Silicate retrieval algorithm

An empirical algorithm was developed by regressing SST, chl-*a* and silicate to create a satellite-based silicate map. To collect *in situ* data, monthly samples were collected from the four sampling stations along SW BoB from 2013 to 2017. The *in situ* SST and chl-*a* datasets were regressed with the silicate in 3-dimensions for four distinct functions, such as plane, paraboloid, Gaussian and Lorentzian functions. In the entire regression analysis, the paraboloid function was found to perform better fit than the other functions and showed good relationship between the variables. The algorithm implies the following equation.

$$\text{Silicate} = 173.6620 - 9.6481 \times \text{SST} + 2.8716 \times \text{chl} + 0.1383 \times \text{SST}^2 - 0.0276 \times \text{chl}^2$$

Where, SST is Sea Surface Temperature and chl is chlorophyll-*a* concentration

### Results and Discussion

During the present study, SST (Fig. 2a) was observed to be high in the summer season, with a

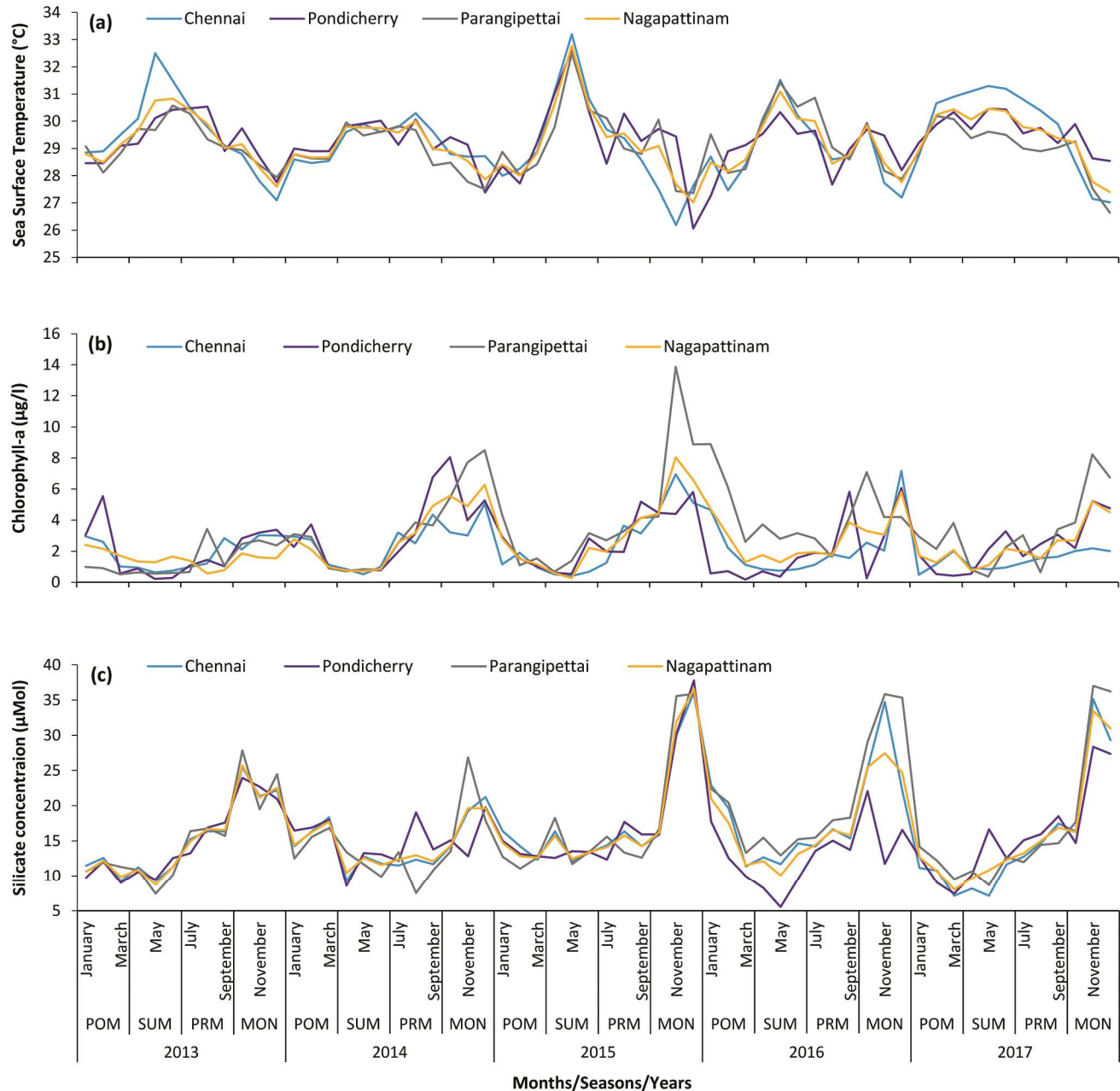


Fig. 2 — Seasonal and inter-annual variation of physico-chemical parameters in the Southwest Bay of Bengal from January 2013 to March 2017 during study period: a) Sea Surface Temperature (SST), b) chlorophyll-*a*, and c) silicate concentration

highest of 33.2 °C at Chennai in the month of May, 2015 and a lowest of 26.0 °C at Cuddalore in the month of December, 2015 *i.e.* in the monsoon season, as the water in the SW BoB is warm in summer and cooled in monsoon. In contrast, the chl-*a* concentration (Fig. 2b) was maximum at Parangipettai region in November, 2015 (13.87 µg/l) *i.e.* in the monsoon season and was minimum (0.27 µg/l) in Nagapattinam region in May, 2015 *i.e.* in the summer

season. Similarly, the silicate concentration ranged from 5.55 to 37.78 µM (Fig. 2c) with highest concentration recorded in the monsoon season (December, 2015) and lowest concentration in the summer season (May, 2016). The increase in chl-*a* concentration coincides with the increased silicate content, implying a positive correlation between chl-*a* and silicate. The presence of adequate UV radiation, river runoff, nutrients, and the consumption of silicate

by diatoms which are enhanced by river flow during the monsoon could all be the contributing factors to the increased level of chlorophyll-*a* concentration during the monsoon season<sup>15-16</sup>. The seasonal variations in the magnitude of the solar radiation and surface winds are causes for the SST fluctuations. Since, weaker winds prevail in the SW BoB in summer and sunlight exposure is stronger owing to the absence of clouds, SST is enhanced over the region<sup>16</sup>. In contrast, the SW BoB experiences cooling in monsoon *i.e.* during the monsoon season due to the strong northeasterly winds, cold sea surface, and cloud cover caused by the northeast monsoon. The correlation study revealed an inverse relationship ( $r = -0.088$ ,  $P < 0.05$ ) among chlorophyll and SST, as reported by Shanthi *et al.*<sup>17</sup>. This is due to the fact that higher SST and light intensity tend to decrease phytoplankton populations, as per the evidence discussed by Hossain *et al.*<sup>18</sup>. Enhancing light condition and high stratification caused by raised surface warming and decreased wind stress during summer affect nutrient delivery to surface water and reduce biological productivity<sup>18-19</sup>. The relationship between chlorophyll concentration and SST are therefore inverse.

However, an inverse relationship between chl-*a* and SST was found to affect phytoplankton biomass<sup>9</sup> resulting in a significant negative correlation with silicate. Nagamani *et al.*<sup>20</sup> have found an inverse relationship between temperature and nutrients<sup>21-22</sup> and also described an inverse correlation between SST and silicate, which is the best fit. These relationships occur, as nutrient-rich cold water present during monsoon mixing becomes gradually warmer with time and as nutrients are taken up by phytoplankton for their growth and development<sup>9</sup>.

Dugdale & Wilerson<sup>1</sup> have explained the significance of understanding the silicate cycling in open-ocean systems and abundant research is underway. The current study, showed a strong positive relationship between silicate and chl-*a*. This technique provided a new solution to determine the distribution of silicate concentration using satellite images such as VIIRS chlorophyll and SST for water bodies.

The silicate concentration is greater than that of any other nutrients in the BoB, as reported by Chavez *et al.*<sup>23</sup>. This may be mainly due to the massive influx of monsoonal water. In coastal waters, the spatio-temporal variation of silicate can be strongly

influenced by a variety of factors, including the physical mixing of freshwater and seawater, chemical reaction with clay minerals, co-precipitation with organic substances, etc. The reactive silicate is adsorbed from the suspended sedimentary particles and then biologically removed by phytoplankton, which includes silicoflagellates and diatoms<sup>7</sup>. Diatoms are predominant in the phytoplankton biomass<sup>24-25</sup>. The growth rates of diatoms are determined by the silicate supply<sup>26</sup>. Diatoms stoichiometrically consume silica in the Redfield ratios of 1:1 atomic ratio with nitrate. For silicates, diatoms are Si-limited at Si:N ratios of 1:1, but N-limited at nitrate (Si:N) supply ratios of  $< 1:1$ <sup>(ref. 27)</sup>. In this context, BoB is a nitrate limited region<sup>4,28</sup>. Silicate and nitrates are essential for diatom development and growth. Moreover, biogenic silicon content was determined based on the diatom percentage within the phytoplankton community and its associated chlorophyll-*a* concentration, under the assumption of similar range of chlorophyll-*a* levels across all phytoplankton groups<sup>29</sup>. To measure the biogenic silicate content from diatoms, the chl-*a* of the diatoms was transformed to carbon (C) units utilizing the C:chl-*a* ratio of 50:1<sup>(ref. 30)</sup> and then transformed to Si moles using the Redfield ratio (C:Si, 106:16)<sup>31</sup>. However, an in-depth understanding of the relationship between silicate concentration and chl-*a* is an essential prerequisite for evaluating the importance of temperature and for developing scientifically sound strategies for creating the silicate algorithm.

The empirical silicate algorithm in the present study was generated using *in situ* observations of SST, chl-*a* and silicate. The regression analysis was performed in three dimensions for plane, paraboloid, Gaussian and Lorentzian functions with regression plots as shown in Figure 3. To facilitate filtering and extrapolation of the data, a best-fit curve for silicate as a function of temperature was defined for each region. Most of the scatter plots showed a non-linear relationship at low temperatures and a linear relationship approaching zero at higher temperatures. The outliers remaining in the dataset were removed as the developed algorithm may adequately reduce the influence of the outlier to obtain better, higher and more accurate values with the Root Mean Square Error (RMSE). The analysis resulted in the following algorithms.

$$\text{Silicate} = 54.3791 - 1.5261 \times \text{SST} + 2.9837 \times \text{chl} \quad \dots \text{Plane}$$

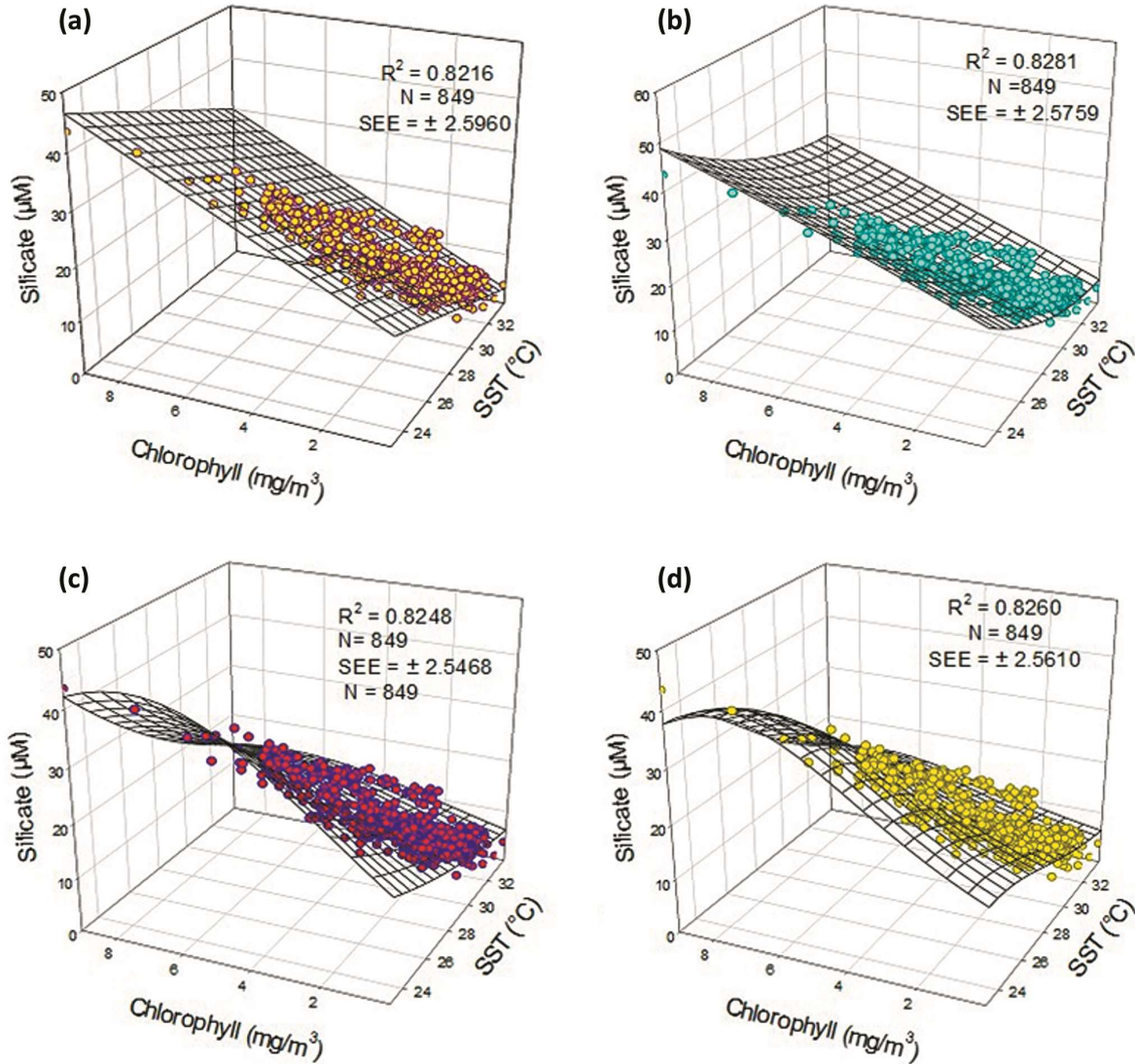


Fig. 3 — Three-dimensionally modeled regression plots for *in situ* SST, chlorophyll-*a* and silicate datasets during 2013 – 17: (a) Plane, (b) Paraboloid, (c) Gaussian, and (d) Lorentzian functions

$$Silicate = 173.6620 - 9.6481 \times SST + 2.8716 \times chl + 0.1383 \times SST^2 - 0.0276 \times chl^2 \quad \dots \text{Paraboloid}$$

$$Silicate = 222.1788 \times \exp \left[ -0.5 \left[ \frac{SST + 13.1394}{20.1315} \right]^2 + \left[ \frac{chl - 7.3247}{5.5337} \right]^2 \right] \quad \dots \text{Gaussian}$$

$$Silicate = \frac{40.5762}{\left[ 1 + \frac{(SST - 23.0380)^2}{-8.2228} \right] \times \left[ 1 + \frac{Chl - 7.3927}{6.3327} \right]^2} \quad \dots \text{Lorentzian}$$

Where, *SST* is Sea Surface Temperature and *chl* is chlorophyll-*a* concentration. All the models

performed well, especially the paraboloid function has obtained better regression ( $R^2 = 0.828$ ,  $N = 849$ ). Of these functions, no separate validation was performed for the current study, and the mapped silicate concentrations were directly incorporated into the paraboloid model as shown in Figure 4. Similar to current study, a high relationship between chl-*a*, SST and silicates in the sea surface region was found in the China Sea<sup>32</sup>. Furthermore, Fu *et al.*<sup>33</sup> reported a linear relationship between *in situ* measured chl-*a* and silicate concentration with an  $R^2$  of 0.781 from East China Sea. Zhang *et al.*<sup>34</sup> also observed a high correlation between chl-*a* and silicates, with a correlation coefficient of 0.808. While comparing Pearson's correlation coefficient between SST and

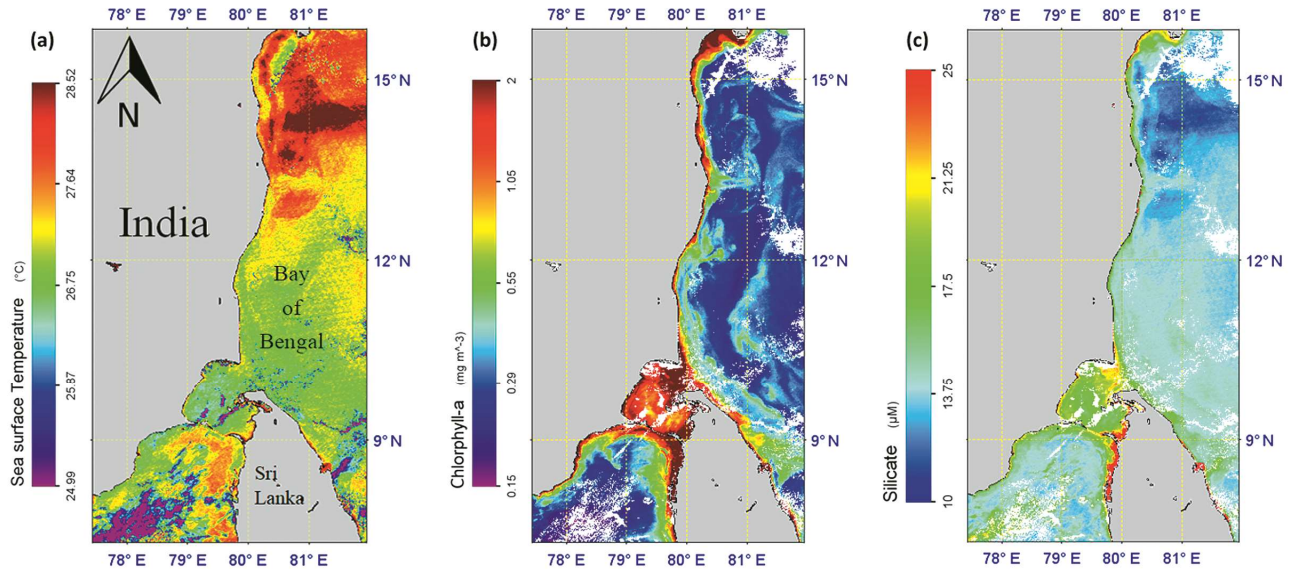


Fig. 4 — (a) VIIRS derived SST, (b) VIIRS derived chlorophyll-*a*, and (c) Modeled silicate image, around SW Bay of Bengal

chlorophyll-*a* concentration (-0.322), it revealed that SST has a more significant impact on nutrient concentration than on phytoplankton growth. However, an inverse correlation between SST and silicates (-0.63) was reported by Tu *et al.*<sup>35</sup>. Similar to previous studies, results of present study showed a high relationship between chl-*a*, SST and silicate concentrations in the SW BoB. Moreover, the silicate algorithm in the region was retrieved with chl-*a* and SST. It was difficult to obtain consecutive cloud free data for SW BoB, hence the validation of VIIRS data was conducted with limited accessible datasets on 31<sup>st</sup> January 2017.

#### Validation of VIIRS derived SST

The validation of the VIIRS-SST with the *in situ* SST (Fig. 5a) showed a good correlation coefficient ( $R^2 = 0.634$ ;  $SEE = \pm 0.227$ ), indicating better retrieval of SST by the VIIRS in the SW BoB. Previously, Tu *et al.*<sup>35</sup> validated VIIRS with eight different kinds of *in situ* SST from five different sources that matched VIIRS SST within  $\pm 1$  h and  $\pm 0.05^\circ$  of latitude and longitude. The results of the present study found high relationships with VIIRS SST, except for Coral Reef Watch (CRW) buoy and an RMSE of  $\leq 0.4$  °C for both day and nighttime. Further, the comparison of the *in situ* SST with the VIIRS SST (Fig. 5b) showed an 80 % underestimation and 20 % overestimation of the *in situ* SST range above the 1:1 line (mean Normalized Bias (MNB) = 0.006 and RMSE = 0.280), with data points falling above or below the 95 % confidence interval. This indicates that the values observed are lower or higher than they

would be in marine waters<sup>36</sup> suggesting a stratification in the surface marine layer combined with weak wind conditions  $< 6$  m/s which might prompt slip-up in the measurements of SST. While, when the wind speed reduces under 6 m/s at the surface of the ocean, the SST estimated by the satellite sensors increases<sup>13,35-36</sup> leading to positive bias SST<sup>13</sup>.

#### Validation of VIIRS derived chlorophyll-*a*

The chlorophyll-*a* determined with VIIRS showed a better agreement with the *in situ* chl-*a* with a correlation coefficient (Fig. 6a) of  $R^2 = 0.523$  with  $SEE = \pm 0.634$ ,  $MNB = 0.369$ , and  $RMSE = 0.846$ . Comparison of the *in situ* chl-*a* with VIIRS derived chlorophyll-*a* estimates shows 40 % overestimation and 60 % underestimation of data points distributed around the 1:1 line (Fig. 6b). In comparison to MODIS, VIIRS demonstrated better geographical coverage and detection accuracy. After enhancing the coefficient, VIIRS shown a 53 % accuracy rate in chl-*a* prediction<sup>37</sup>. The water leaving radiance between *in situ* and VIIRS data was found to have excellent matching, as validated by an inter-comparison of the VIIRS ocean colour products with *in situ* observations<sup>38</sup>. Hlaing<sup>39</sup> also included preliminary assessments of the performance of the VIIRS sensor for obtaining ocean colour information of typical coastal water by performing initial time series and qualitative and quantitative correlation studies between *in situ* and satellite-based ocean colour information. An important component of the entire strategy for the validation and calibration of satellite

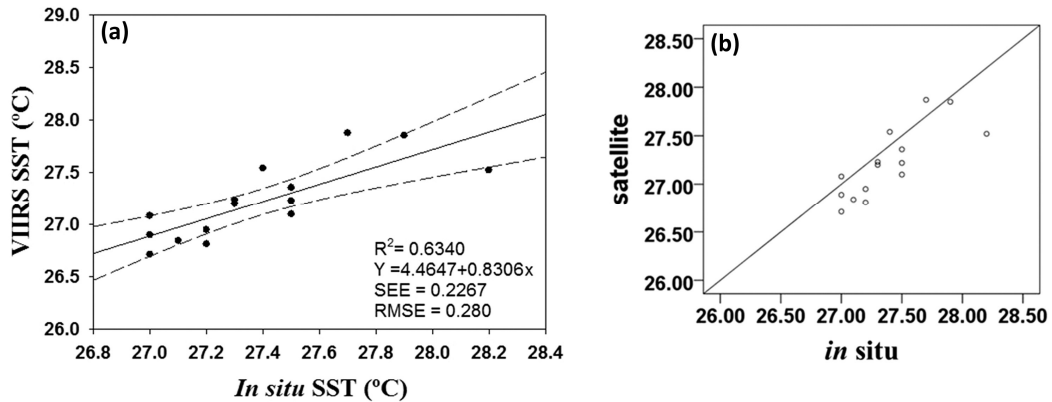


Fig. 5 — (a) Regression, and (b) comparison plot of *in situ* vs VIIRS derived SST

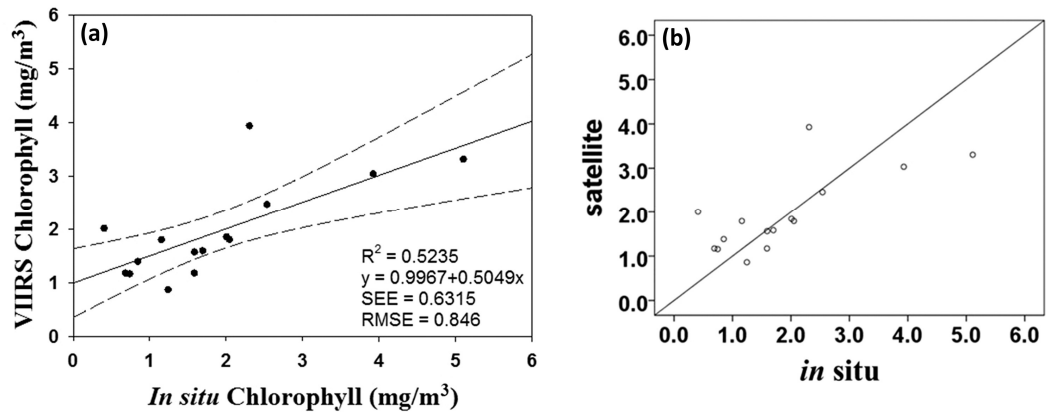


Fig. 6 — (a) Regression, and (b) comparison plot of *in situ* vs VIIRS derived chlorophyll-*a*

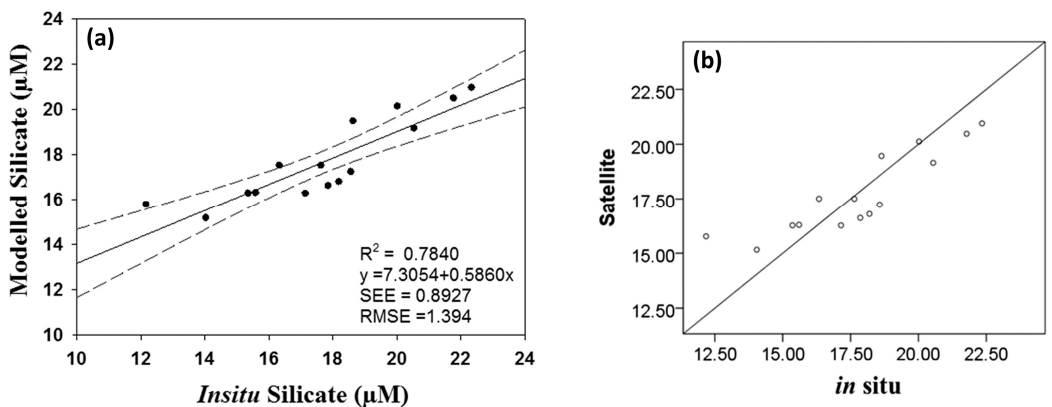


Fig. 7 — (a) Regression, and (b) comparison analysis of *in situ* silicate vs modeled silicate

imagery (VIIRS) is the confirmation that the image data is appropriate for efficient operational application<sup>40</sup>.

**Validation of SST and chlorophyll-*a* based silicate algorithm**

The assessments of the output of the silicate algorithm was based on the statistical parameters of the comparison of the satellite-derived silicate values with the *in situ* silicate values. The silicate map

derived from the algorithm provides a better retrieval of silicate in the SW BoB with a correlation coefficient (Fig. 7a) of  $R^2 = 0.784$  with *in situ* silicate. The developed silicate algorithm tested using the *in situ* values showed a quite small systematic error, with a calculated value of  $MNB = -0.008$ . However, there was considerable scatter in the matching points. The RMSE, which is a measure of dispersion, was 1.394 and SEE was  $\pm 0.893$ . The comparison plot

(Fig. 7b) shows the uniform distribution of the points around the 1:1 line without distinct trends of either under or overestimation of VIIRS retrieved silicate with *in situ* silicate estimates that portray 47 % overestimation and 53 % underestimation. The validation of the empirical silicate algorithm found statistically significant while comparing silicate with *in situ* VIIRS derived SST and chl-*a*. Many more measurements of SST, chl-*a* and silicate by collecting more global ocean data would help to further improve the algorithm and future predictions.

### Acknowledgements

We thank Dean and Director, CAS in Marine Biology, Annamalai University. This work is supported by Space Application Centre (SAC), ISRO, Government of India, Ahmedabad. We are also thankful to the anonymous reviewers for their suggestions and comments.

### Funding

Meteorology and Oceanography (MOP-2) Program of ISRO (MOP-II), Ministry of Earth Sciences, India.

### Conflict of Interest

The authors declare no conflict of interest.

### Author Contributions

KP: Overall preparation of the manuscript and data analysis; RKS & RS: Designing of the study, review and editing; DLA: Software; RKS: Funding acquisition; and AS: Resources, supervision, administration, and visualization.

### References

- Dugdale R C & Wilerson F P, Silicate regulation of new production in the equatorial Pacific upwelling, *Nature*, 391 (1998) 270-273. <https://doi.org/10.1038/34630>
- Sarangi R K, Thangaradjou T, Poornima D, Shanthi R, Kumar A S, *et al.*, Seasonal nitrate algorithms for the SW Bay of Bengal water using *in situ* measurements for satellite remote-sensing applications, *J Coast Res*, 31 (2) (2015) 398-406. <https://doi.org/10.2112/JCOASTRES-D-12-00270.1>
- Treguer P & Pondaven P, Silica control of carbon dioxide, *Nature*, 406 (2000) 358-359. <https://doi.org/10.1038/35019236>
- Thangaradjou T, Sarangi R K, Shanthi R, Poornima D, Raja K, *et al.*, Changes in nutrients ratio along the central Bay of Bengal coast and its influence on chlorophyll distribution, *J Environ Biol*, 35 (3) (2014) 467-477.
- Lewin J C, Silicification, In: *Physiology and Biochemistry of Algae*, edited by Lewin R A, (Academic Press, New York), 1962, pp. 445-455.
- Conley D J & Malone T C, Annual cycle of dissolved silicate in Chesapeake Bay: Implications for the production and Fate of Phytoplankton biomass, *Mar Ecol Prog Ser*, 81 (1992) 121-128. <https://doi.org/10.3354/meps081121>
- Satpathy K K, Mohanty A K, Natesan U & Sarkar S K, Seasonal variation in physicochemical properties of coastal waters of Kalpakkam, east coast of India with special, *Environ Monit Assess*, 164 (2010) 153-171. <https://doi.org/10.1007/s10661-009-0882-0>
- Thangaradjou T, Sethubathi G V, Raja S, Poornima D, Shanthi R, *et al.*, Influence of environmental variables on phytoplankton floristics pattern along the shallow coasts of SW Bay of Bengal, *Algal Res*, 1 (2) (2012) 143-154. <https://doi.org/10.1016/j.algal.2012.07.005>
- Henson S A, Sanders R, Holeton C & Allen J T, Timing of nutrient depletion diatom dominance and a lower-boundary estimate of export production for Irminger Basin, North Atlantic, *Mar Ecol Prog Ser*, 313 (2006) 73-84. <http://dx.doi.org/10.3354/meps313073>
- Balachandran K K, Laluraj C M, Jyothibabu R, Madhu N V, Muraliedharan K R, *et al.*, Hydrography and biogeochemistry of the north western Bay of Bengal and the north eastern Arabian Sea during winter monsoon, *J Mar Syst*, 73 (1-2) (2008) 76-86. <https://doi.org/10.1016/j.jmarsys.2007.09.002>
- Balakrishnan S, Chelladuran G, Mohanraj J & Poongodi J, Seasonal variation in physico-chemical characteristics of Tuticorin coastal waters, southeast coast of India, *Appl Water Sci*, 7 (4) (2017) 1881-1886. <https://doi.org/10.1007/s13201-015-0363-2>
- Sarangi R K, Thangaradjou T, Kumar A S & Balasubramanian T, Development of nitrate algorithm for the Southwest Bay of Bengal water and its implication using remote sensing satellite datasets, *IEEE J Sel Top Appl Earth Obs Remote Sens*, 4 (4) (2011) 983-991. <https://doi.org/10.1109/JSTARS.2011.2165204>
- Poornima D, Sarangi R K, Shanthi R, Thangaradjou T & Prakash C, Seasonal nitrate algorithms for nitrate retrieval using OCEANSAT-2 and MODIS-AQUA satellite data, *Environ Monit Assess*, 187 (2015) 1-15. <https://doi.org/10.1007/s10661-015-4340-x>
- Parsons T R, Maita Y & Lalli C M, Determination of Silicate, In: *A Manual of Chemical and Biological Methods for Seawater Analysis*, (Pergamon Press, Oxford, New York), 1984, pp. 25-28. <http://dx.doi.org/10.25607/OBP-1830>
- Prabhakar C, Saleshrani K, Dhanasekaran D, Tharmaraj K & Baskaran K, Seasonal variations in physico-chemical parameters of Nagapattinam Coastal area, Tamil Nadu, India, *Int J Curr Life Sci*, 1 (6) (2011) 29-32.
- Sardessai S, Ramaiah N, Kumar P S & De Souza S N, Influence of environmental forcing on the seasonality of dissolved oxygen and nutrients in the Bay of Bengal, *J Mar Res*, 65 (2) (2007) 301-316. <http://drs.nio.org/drs/handle/2264/623>
- Shanthi R, Poornima D, Raja K, Sarangi R K, Saravanakumar A, *et al.*, Inter-annual and seasonal variations in hydrological parameters and its implications on chlorophyll a distribution along the southwest coast of Bay of Bengal, *Acta Oceanolog Sin*, 34 (6) (2015) 94-100. <https://doi.org/10.1007/s13131-015-0689-5>
- Hossain M Y, Jasmine S, Ibrahim A H M, Ahmed Z F, Ohtomi J, *et al.*, A preliminary observation on water quality

- and plankton of an earthen Fish Pond in Bangladesh: recommendations for future studies, *Pakistan J Biol Sci*, 10 (6) (2007) 868–873. <https://doi.org/10.3923/pjbs.2007.868.873>
- 19 Kumar S P, Muraleedharan P M, Prasad T G, Ganus M, Ramaiah N, *et al.*, Why is the Bay of Bengal less productive during summer monsoon compared to the Arabian Sea? *Geophys Res Lett*, 29 (24) (2002) p. 2235. <https://doi.org/10.1029/2002GL016013>
  - 20 Nagamani P V, Shikhakolli R & Chauhan P, Phytoplankton variability in the Bay of Bengal during winter monsoon using Oceansat-1 Ocean Colour Monitor data, *J Indian Soc Remote Sens*, 39 (1) (2011) 117–126. <https://doi.org/10.1007/s12524-010-0056-0>
  - 21 Kamykowski D & Zentara S J, Predicting plant nutrient concentrations from temperature and sigma-t in the upper kilometer of the world ocean, *Deep-Sea Res I: Oceanogr Res Pap*, 33 (1) (1986) 89-105. [https://doi.org/10.1016/0198-0149\(86\)90109-3](https://doi.org/10.1016/0198-0149(86)90109-3)
  - 22 Manasrah R, Raheed M & Badran M I, Relationships between water temperature, nutrients and dissolved oxygen in the northern Gulf of Aqaba, Red Sea, *Oceanologia*, 48 (2) (2006) 237-253. <http://water.iopan.gda.pl/oceanologia/482manas.pdf>
  - 23 Chavez F P, Service S K & Buttrely S E, Temperature-nitrate relationships in the central and eastern tropical Pacific, *J Geophys Res Oceans*, 101 (C9) (1996) 20553-20563. <https://doi.org/10.1029/96JC01943>
  - 24 Eppley R W, Temperature and Phytoplankton growth in the Sea, *Fish Bull*, 70 (4) (1972) 1068-1085.
  - 25 Yoder J, Effect of Temperature on Light-Limited Growth and Chemical composition of *Skeletonema Costatum* (Bacillariophyceae), *J Phycol*, 15 (4) (1979) 363-370. <https://doi.org/10.1111/j.1529-8817.1979.tb00706.x>
  - 26 Ittekkot V, Humborg C & Schafer P, Hydrological Alterations and Marine Biogeochemistry: A Silicate Issue? Silicate retention in reservoirs behind dams affects ecosystem structure in coastal seas, *Bio Sci*, 50 (9) (2000) 776-782. <https://doi.org/10.1641/0006-3568>
  - 27 Smayda T J, Eutrophication and phytoplankton, In: *Drainage Basin Nutrient Inputs and Eutrophication: An Integrated Approach*, edited by Wassmann P & Olli K, (University of Tromso, Norway), 2004, pp. 89-98. ISBN: 82-910866-94-2
  - 28 Paul J T, Ramaiah N & Sardessai S, Nutrient regimes and their effect of distribution of phytoplankton in the Bay of Bengal, *Mar Environ Res*, 66 (3) (2008) 337-344. <https://doi.org/10.1016/j.marenvres.2008.05.007>
  - 29 Sospedra J L, Niencheski F H, Falco S, Andrade C F F, Attisano K K, *et al.*, Identifying the main sources of silicate in coastal waters of the Southern Gulf of Valencia (Western Mediterranean Sea), *Oceanologia*, 60 (1) (2018) 52-64. <https://doi.org/10.1016/j.oceano.2017.07.004>
  - 30 Ciotti A M, Odebrecht C, Fillmann G & Moller O O, Freshwater outflow and Subtropical Convergence influence on phytoplankton biomass on the southern Brazilian continental shelf, *Cont Shelf Res*, 15 (14) (1995) 1737-1756. [https://doi.org/10.1016/0278-4343\(94\)00091-Z](https://doi.org/10.1016/0278-4343(94)00091-Z)
  - 31 Redfield A C, Ketchum B H & Richards F A, The influence of organisms on the composition of sea-water, In: *The composition of seawater: Comparative and descriptive oceanography. The sea: ideas and observations on progress in the study of the seas*, Vol 2, edited by Hill M N, (Wiley-Inter science, New York), 1963, pp. 26-77.
  - 32 Chen C T A, Chemical and physical fronts in the Bohai, Yellow and East China seas, *J Mar Syst*, 78 (3) (2009) 394–410. <https://doi.org/10.1016/j.jmarsys.2008.11.016>
  - 33 Fu D, Huang Z, Zhang Y, Pan D, Ding Y, *et al.*, Factors affecting spring bloom in the South of Cheju island in the east China sea, *Acta Oceanolog Sin*, 34 (2015) 51–58. <https://doi.org/10.1007/s13131-015-0633-8>
  - 34 Zhang Y, Huang Z, Fu D, Tsou J Y, Jiang T, *et al.*, Monitoring of chlorophyll-*a* and sea surface silicate concentrations in the south part of Cheju island in the East China sea using MODIS data, *Int J Appl Earth Obs Geoinf*, 67 (2018) 173–178. <https://doi.org/10.1016/j.jag.2018.01.017>
  - 35 Tu Q, Pan D & Hao, Validation of S-NPP VIIRS Sea Surface Temperature Retrieved from NAVO, *Remote Sens*, 7 (12) (2015) 17234-17245. <https://doi.org/10.3390/rs71215881>
  - 36 Donlon C J, Minnett P J, Gentemann C, Nightingale T J, Barton I J, *et al.*, Toward improved validation of satellite sea surface skin temperature measurements for climate research, *J Clim*, 15 (4) (2002) 353-369. [https://doi.org/10.1175/1520-0442\(2002\)015%3C0353:TIVOSS%3E2.0.CO;2](https://doi.org/10.1175/1520-0442(2002)015%3C0353:TIVOSS%3E2.0.CO;2)
  - 37 Zeng C, Xu H & Fischer A M, Chlorophyll-*a* Estimation around the Antarctica Peninsula Using Satellite Algorithms: Hints from field water leaving reflectance, *Sensors*, 16 (12) (2016) 1-14. <https://doi.org/10.3390/s16122075>
  - 38 Arnone R, Fargion G, Martinolich P, Ladner S, Lawson A, *et al.*, Validation of the VIIRS Ocean Color, *Proc SPIE 8372, Ocean Sens Monit IV, 83720G*, 12 June 2012, 2012, pp. 10. <https://doi.org/10.1117/12.922949>
  - 39 Hlaing S, Harmel T, Gilerson A, Foster R, Weidemann A, *et al.*, Evaluation of the VIIRS ocean color monitoring performance in coastal regions, *Remote Sens Environ*, 139 (2013) 398-414. <https://doi.org/10.1016/j.rse.2013.08.013>
  - 40 Hillger D, Kopp T, Seaman C, Miller S, Lindsey D, *et al.*, User Validation of VIIRS Satellite Imagery, *Remote Sens*, 8 (1) (2016) 1-11. <https://doi.org/10.3390/rs8010011>